Effect of Incompressibility and Symmetry Energy Density on Charge Distribution and Radii of Closed-Shell Nuclei

Shayma'a H. Amin[1]*, Ahmed A. Al-Rubaiee[2], Ali H. Taqi [3]

[1*,2] *Department of Physics, College of Science, Al-Mustansiriyah University, Baghdad, Iraq.*
[3] *Department of Physics, College of Science, Kirkuk University, Kirkuk, Iraq.*
***Corresponding author**: shaymaahussein7988@yahoo.com.

Article Information:

History:
Received: 20 August 2022.
Accepted: 25 September 2022.
Published: 30 September 2022.

Keywords:
Hartree-Fock HF; Skyrme interaction; Charge distribution; Root-mean-square radii.

DOI:http://dx.doi.org/110.32894/kujss.2022.135889.1073

Abstract

In this work, the effect of incompressibility modulus K_{NM} and symmetry energy density J on charge distribution and root-mean-square radii of neutron R_n and proton R_p has been investigated for light, medium and heavy closed-shell nuclei ${}^{40}_{20}Ca_{20}$, ${}^{48}_{20}Ca_{28}$, ${}^{90}_{40}Zr_{50}$, ${}^{116}_{50}Sn_{66}$, ${}^{144}_{62}Sm_{82}$ and ${}^{208}_{62}Pb_{126}$ within the framework of self-consistent Hartree-Fock (HF) with 20 types of Skyrme interactions having wide range of nuclear properties such as incompressibility modulus K_{NM} and symmetry energy density J. The nuclear charge densities have been obtained and compared with the experiment data to give us a picture about the internal structure of the investigated nuclei. Also, the relation between the proton and neutron root-mean-square radii, and nuclear matter properties has been studied and examined by determining and discussion the statistical Pearson linear correlation coefficient, to help in formulating nuclear interaction.

1. Introduction:

The main problem in physics is many-body problem [1], In nuclear physics, the many-body systems and the nature of the nuclear force [2] are the most important challenges facing physics the theoretical nuclear physics, therefore, theoretical researches in nuclear physics aim to describe the structure of the nuclei with a universal nuclear model.

The properties of ground-state of atomic nuclei can be studied by Hartree-Fock (HF) [3], [4] or Hartree-Fock- Bogoliubov [5], [6]. There are many models used to study the excited levels, and the Random Phase Approximation (RPA) is considered successful in studying the closed-shell nuclei [7]. Charge density distribution and radii are fundamental nuclear properties applied to probe the nucleus structure and describes the effect of effective interactions on nuclear structure [8], [9] which were measured by electron elastic scattering and muonic X-ray data [10] by methods based on the electromagnetic interaction between the nucleus and electrons or muons.

It has also been indicated by many research groups that the nuclear properties are closely related to the symmetry term of the equation of state (EOS) [11], [12]. Charge radii is a good indicator of nuclear properties and the nuclear symmetry energy that characterizes the equation of state of matter [13], also, it found correlates strongly with other observables in nuclei, such as nuclear charge and radii [14],[15],[16], or neutron skin thickness [17],[18],[19], and their relationship to the nuclear matter properties [20],[21]. The present work aims to study the effect of incompressibility modulus K_{NM} and symmetry energy density J on charge distribution and root-mean-square radii of neutron (R_n) and proton (R_p) for light, medium and heavy closed-shell nuclei ${}^{40}Ca$, ${}^{48}Ca$, ${}^{90}Zr$, ${}^{116}Sn$, ${}^{144}Sm$ and ${}^{208}Pb$ using the self-consistent Hartree-Fock (HF) with 20 types of Skyrme interactions. Having a large number of Skyrme-force parameterizations requires continuous search for the best to describe the experimental data, therefore, the nuclear charge densities to be obtained and compared with the experiment data to give us an imagination about the internal structure of the investigated nuclei, as well as, the dependence of proton and neutron root-mean-square radii to nuclear matter properties such as incompressibility modulus K_{NM} and symmetry energy density J to be examined by determining the statistical Pearson linear correlation coefficient.

2. Theoretical framework:

The second quantization Hamiltonian of a many-body fermion system is a summation of the kinetic energy t is and the anti-symmetrized two body matrix-elements $\bar{v}_{n\acute{n}m\acute{m}} = (k_n k_{\acute{n}}|V|k_m k_{\acute{n}} - k_{\acute{m}} k_m)$ as given below [22],

$$H = \sum_{n\acute{n}} t_{n\acute{n}} \hat{c}^{\dagger}_{\acute{n}} \hat{c}_{\acute{n}} + \frac{1}{4} \sum_{n\acute{n}m\acute{m}} \bar{v}_{n\acute{n}m\acute{m}} \hat{c}^{\dagger}_{n} \hat{c}^{\dagger}_{\acute{n}} \hat{c}_{m} \hat{c}_{\acute{m}} \quad (1)$$

Where $\hat{c}$ and $\hat{c}^{\dagger}$ are annihilation and creation operators, respectively with $\hat{c}|\rangle = 0$. The indices: $n, \acute{n}, m, \acute{m}$ covers all degrees of freedom of all available single particle states.

The Hartree-Fock energy can be expressed as,

$$E^{HF} = \sum_{nn'} t_{nn'} \rho_{n'n} + \frac{1}{2} \sum_{nn'mm'} \rho_{nm} V_{nn'mm'} \rho_{m'n'} \quad (2)$$

where single-particle density ρ is diagonal which has the eigenvalues 1 or 0 for occupied and non-occupied states, and the energy should be minimized to determine the HF-basis [22],

$$h^{HF}_{nn'} = t_{nn'} + \Gamma_{nn'}(\rho) \quad (3)$$

with the self-consistent field.

$$\Gamma_{nn'}(\rho) = \sum_{mm'} V_{nn'mm'} \rho_{n'm'} \quad (4)$$

The Skyrme effective interaction [23], [24] is one of the most convenient forces used in HF calculations to describe the nuclear properties in ground-state, commonly contains central, non-local and density-dependent terms [25], [26]:

$$\begin{aligned} V(r_1, r_2) &= t_0(1 + x_0 P_\sigma)\delta(r_1 - r_2) \\ &+ \frac{1}{2} t_1 (1 + x_1 P^{\alpha}_{12}) \times [\vec{k}^2_{12} \delta(r_1 - r_2) + \delta(r_1 - r_2)\vec{k}^2_{12}] \\ &+ t_2 (1 + x_2 P^{\alpha}_{12}) \overleftarrow{k}_{12} \delta(r_1 - r_2) \vec{k}_{12} \\ &+ \frac{1}{6} t_3 (1 + x_3 P^{\alpha}_{12}) \rho^{\alpha}(R) \delta(r_1 - r_2) \\ &+ \mathrm{i} W_0 \overleftarrow{k}_{12} \delta(r_1 - r_2)(\vec{\sigma}_1 + \vec{\sigma}_2) \vec{k}_{12} \end{aligned} \quad (5)$$

where $\overleftarrow{k}_{12} = -\frac{i(\vec{\nabla}_1 - \vec{\nabla}_2)}{2}, \vec{k}_{12} = -\frac{i(\overleftarrow{\nabla}_1 - \overleftarrow{\nabla}_2)}{2}, P^{\alpha}_{12}$ is the spin-exchange operator and σ_i is the Pauli spin operator.

The Skyrme energy-density functional H(r) contains many terms and given by [27],

$$H = K + H_0 + H_3 + H_{eff} + H_{fin} + H_{so} + H_{sg} + H_{coul} \quad (6)$$

Where K is a kinetic-energy term, H_0 is a zero-range term, H_3 is a density-dependent term, H_{eff} is an effective-mass term, H_{fin} is a finite-range term, H_{sois} a spin-orbit term, H_{sg} is a tensor coupling with spin and gradient term and H_{coul} is a Coulomb interaction term. The charge density distribution in ground-state (in terms of Skyrme HF radial wave function u of the state nlj and occupation probability) can be obtained by [28], [29].

$$\rho_q(r) = \frac{1}{4\pi} \sum_{nlj} \eta_q (2J+1) \left| \frac{u(nlj)}{r} \right|^2 \quad (7)$$

The root-mean-square (rms) radii is defined as,

$$r_q = \sqrt{\langle r^2_q \rangle} = \left[\int r^2 \rho_q(r) dr \Big/ \int \rho_q(r) dr \right]^{1/2} \quad (8)$$

$$\langle r^2_{ch} \rangle = \langle r^2_p \rangle + \langle r \rangle^2_p; \quad rms \quad radius \langle r \rangle_p = 0.8 fm \quad (9)$$

3. Result and discussion:

In this work, The HF calculations have been investigated for ^{40}Ca, ^{48}Ca, ^{90}Zr, ^{116}Sn, ^{144}Sm and ^{208}Pb nuclei by solving the equations numerically with 20 Skyrme-type interaction: SkM^* [30], SQMC650 [31], SV-K218 [32], SQMC700 [31], SkO [33], NRAPR [34], [35], T31 [36], $Sk\chi m$ [37], v075 [38], SkSC10 [39], RATP [40], SAMi [41], SK255 [42], SkD [43], GS2 [44], SIV [45], QMC2 [46], SIII [44], SVII [47]) the meaning of the abbreviation for each type of interaction and its parameters can be found in the cited references). Nuclear matter properties of the used Skyrme interaction such as the incompressibility modulus K_{NM} (MeV) and the symmetry energy density J (MeV), are presented in Table 1. Our results are consistent with those of HFB calculations [5],[6].

The nuclear charge densities have been obtained and compared with the experiment data to give us a picture about the internal structure of the investigated. Figs.(1, 2, 3 and 4) show the calculated HF charge distribution for ^{40}Ca and ^{48}Ca. Good agreements were obtained between our HF results for all of the used types of Skyrme interaction with the experimental data [8],[49] at the surface and interior regions, while our results underestimated the experimental data line inside the investigated nuclei SVII, SIII, QMC2 and GS2 sets.

For ^{90}Zr, our results of charge distribution for all interactions were in a good agreement with the experimental data [8],[50] in the center and at the surface of the nucleus but not so good inside the nucleus as GS2, QMC2 and SVII interactions underestimated the experimental data line inside the nucleus and SQMC650, SQMC700, NRAPR, $Sk\chi$m, SK255, T31, SAMi, RATP parameters in less overestimated the experimental data line inside the nucleus. There are many factors that control the success of the theoretical model, in Table 1, we notice that the value of K_{NM} for the first group is higher than that of the second group.

Table 1. Nuclear matter properties of the used Skyrme interactions [48].

Type	Incompressibility Modulus $K_{NM}(MeV)$	Symmetry Energy Density J(MeV)
SkM*	216.610	30.03
SQMC650	218.110	33.65
SV-K218	218.230	30.00
SQMC700	222.200	33.47
SkO	223.340	31.97
NRAPR	225.700	32.78
KDE0	228.820	33.00
T31	230.010	32.00
$Sk\chi m$	230.400	30.94
v075	231.290	28.00
SkSC10	235.890	22.83
RATP	239.520	29.26
SAMi	245.000	28.00
SK255	254.930	37.40
SkD	267.154	30.81
GS2	300.140	25.96
SIV	324.550	31.22
QMC2	330.100	28.70
SIII	355.370	28.16
SVII	366.440	26.96

For ^{116}Sn, our results of charge distribution for all interactions were in a good agreement with the experimental data [8] in the center and at the surface of the nucleus but not so good inside the nucleus as in SQMC650, SKO, $Sk\chi$m parameters in less overestimated the experimental data line inside the nucleus and GS2, QMC2, SIII and SVII interactions underestimated the experimental data line inside the nucleus. The differences in describing data may due to differences in nuclear properties such as K_{NM}, where its value the first group is lower than of the second group.

For ^{144}Sm our results of charge distribution for all interactions were in a good agreement with the experimental data [8] at the surface of the nucleus but not so good inside the nucleus.

For ^{208}Pb our results of charge distribution for all interactions were in a good agreement with the experimental data [8] in the center and at the surface of the nucleus but not so good inside the nucleus as GS2, QMC2 and SVII and less for SIV and SIII interactions underestimated the experimental data line inside the nucleus and SQMC650, KDE0 parameters in less overestimated the experimental data line inside the nucleus. This may be due to differences in the nuclear matter properties of the investigated types of Skyrme interaction. By considering a light, medium and heavy nuclei, we can illustrate the impact of the effect of incompressibility modulus K_{NM} and symmetry energy density J on root-mean-square radii of neutron R_n and proton R_p for light, medium and heavy closed-shell nuclei $^{40,48}Ca$, ^{90}Zr, ^{116}Sn, ^{144}Sm and ^{208}Pb.

For ^{116}Sn, our results of charge distribution for all interactions were in a good agreement with the experimental data [8] in the center and at the surface of the nucleus but not so good inside the nucleus as in SQMC650, SKO, $Sk\chi$m parameters in less overestimated the experimental data line inside the nucleus and GS2, QMC2, SIII and SVII interactions underestimated the experimental data line inside the nucleus. The differences in describing data may due to differences in nuclear properties such as K_{NM}, where its value the first group is lower than of the second group.

For ^{144}Sm our results of charge distribution for all interactions were in a good agreement with the experimental data [8] at the surface of the nucleus but not so good inside the nucleus.

For ^{208}Pb our results of charge distribution for all interactions were in a good agreement with the experimental data [8] in the center and at the surface of the nucleus but not so good inside the nucleus as GS2, QMC2 and SVII and less for SIV and SIII interactions underestimated the experimental data line inside the nucleus and SQMC650, KDE0 parameters in less overestimated the experimental data line inside the nucleus. This may be due to differences in the nuclear matter properties of the investigated types of Skyrme interaction. By considering a light, medium and heavy nuclei, we can illustrate the impact of the effect of incompressibility modulus K_{NM} and symmetry energy density J on root-mean-square radii of neutron R_n and proton R_p for light, medium and heavy closed-shell nuclei $^{40,48}Ca$, ^{90}Zr, ^{116}Sn, ^{144}Sm and ^{208}Pb.

In Fig.5 the incompressibility K_{NM} are shown as function of R_n and R_p for ^{40}Ca, ^{48}Ca, ^{90}Zr, ^{116}Sn, ^{144}Sm and ^{208}Pb nuclei respectively. the linear correlation coefficients of K_{NM} versus R_n, within the Skyrme forces were 0.395, 0.369, 0.512*, 0.515*, 0.605** and 0.544* for ^{40}Ca, ^{48}Ca, ^{90}Zr, ^{116}Sn, ^{144}Sm and ^{208}Pb nuclei, respectively, where it is small (weak) in ^{40}Ca and ^{48}Ca. The linear correlation coefficients of K_{NM} versus R_p within the Skyrme forces reaches 0.378, 0.489*, 0.552*, 0.562*, 0.591* and 0.606** for ^{40}Ca, ^{48}Ca, ^{90}Zr, ^{116}Sn, ^{144}Sm and ^{208}Pb nuclei, respectively, also it is small (weak) in ^{40}Ca and ^{48}Ca. From Fig.5, we conclude there is an impact of the incompressibility K_{NM} on R_n and R_p.

In Fig.6, the symmetry energy density J are shown as function of R_n and R_p for ^{40}Ca, ^{48}Ca, ^{90}Zr, ^{116}Sn, ^{144}Sm and ^{208}Pb nuclei respectively within the Skyrme forces,

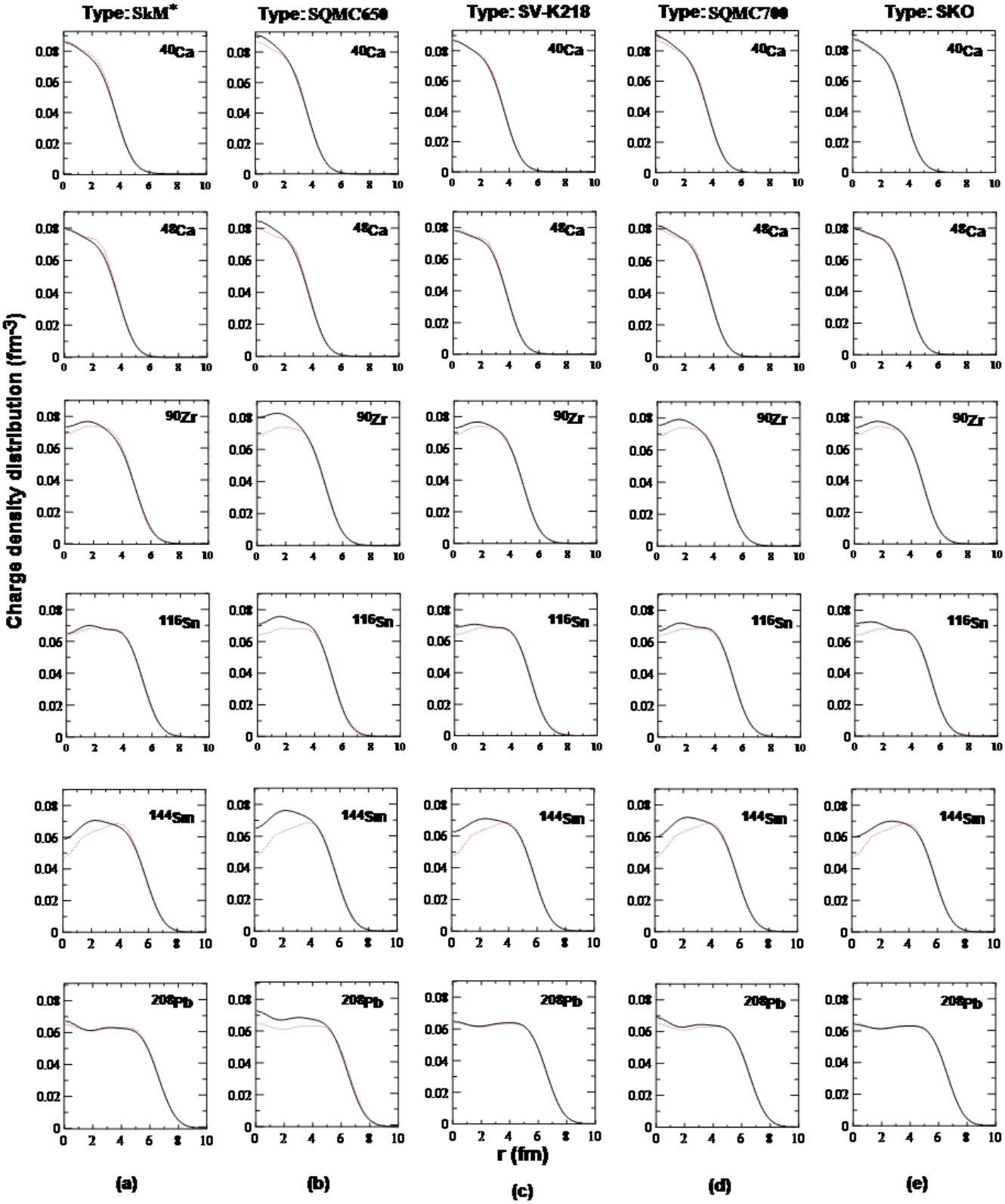

Figure 1. Our obtained charge density distribution (fm^{-3}) of ^{40}Ca, ^{48}Ca, ^{90}Zr, ^{116}Sn, ^{144}Sm and ^{208}Pb nuclei with Skyrme interactions Skm^*, SQMC650, SV-K218, SQMC700, SKO. Charge densities are plotted by black solid line. The red dotted line shows experimental data taken from Ref [8].

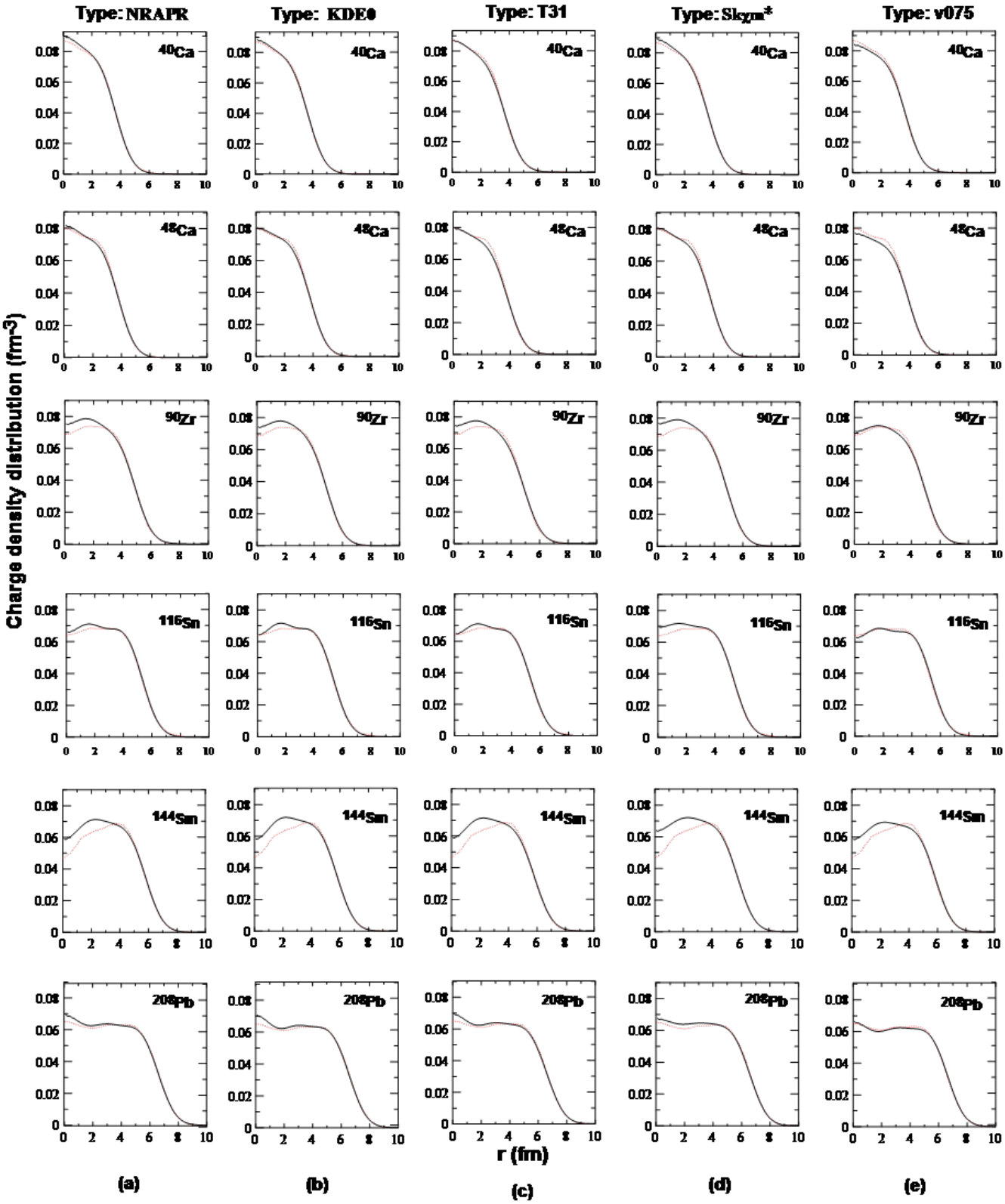

Figure 2. Our obtained charge density distribution (fm^{-3}) of ^{40}Ca, ^{48}Ca, ^{90}Zr, ^{116}Sn, ^{144}Sm and ^{208}Pb nuclei with Skyrme interactions NRAPER, KDE0, T31 $Sk\chi$m and v075. Charge densities are plotted by black solid line. The red dotted line shows experimental data taken from Ref. [8].

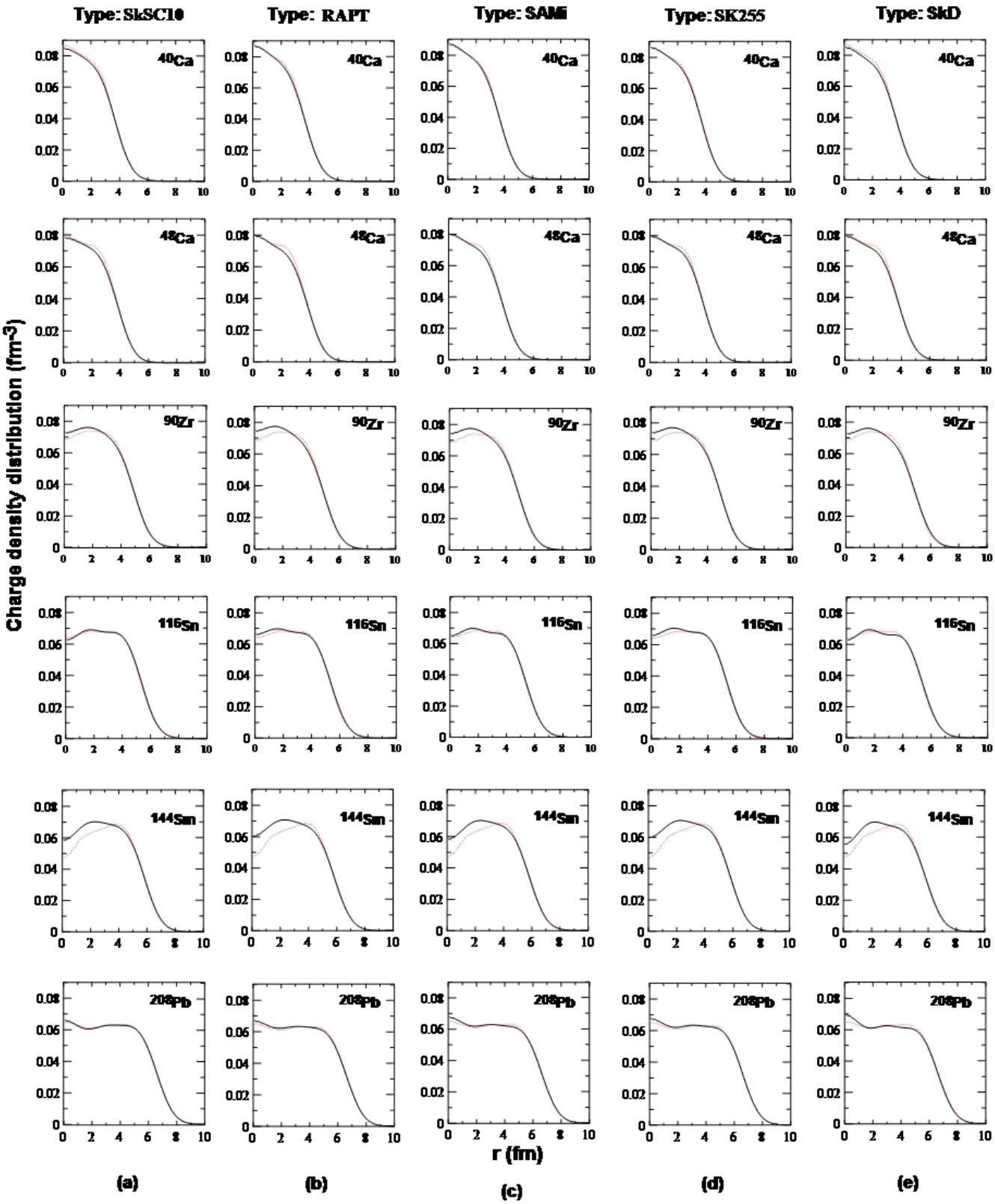

Figure 3. Our obtained charge density distribution (fm^{-3}) of ^{40}Ca, ^{48}Ca, ^{90}Zr, ^{116}Sn, ^{144}Sm and ^{208}Pb nuclei with Skyrme interactions SKSC10, RATP, SAMi, SK255 and SKD. Charge densities are plotted by black solid line. The red dotted line shows experimental data taken from Ref.[8].

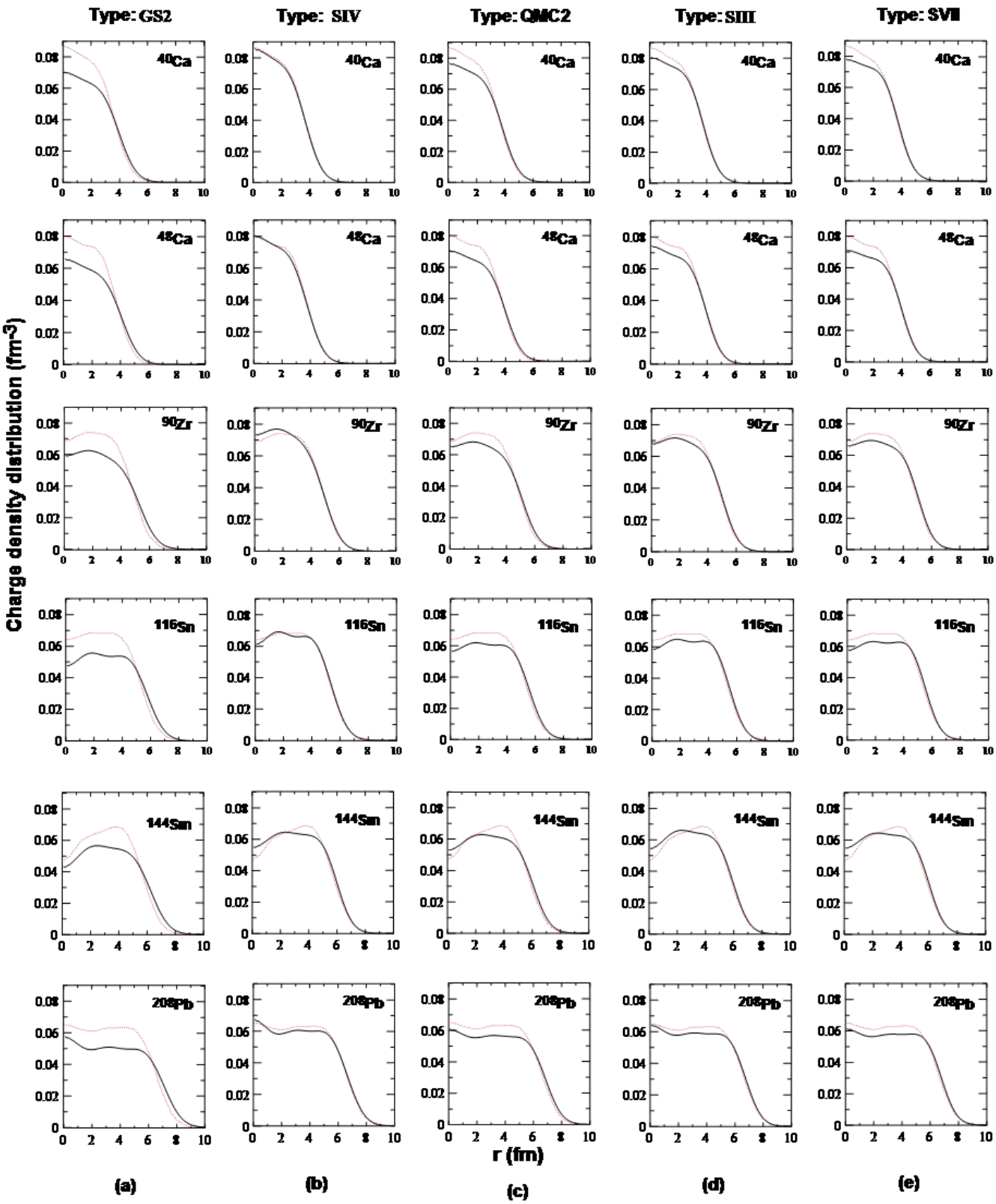

Figure 4. Our obtained charge density distribution (fm^{-3}) of ^{40}Ca, ^{48}Ca, ^{90}Zr, ^{116}Sn, ^{144}Sm and ^{208}Pb nuclei with Skyrme interactions GS2, SIV, QMC2, SIII and SVII. Charge densities are plotted by black solid line. The red dotted line shows experimental data taken from Ref.[8].

the linear correlation coefficients of J versus R_n were -0.433-, -0.179-, -0.308-, -0.254-, -0.212- and -0.032- for ^{40}Ca, ^{48}Ca, ^{90}Zr, ^{116}Sn, ^{144}Sm and ^{208}Pb nuclei, respectively and it is very small correlated except for ^{40}Ca it is rather better than other. The linear correlation coefficients of J versus R_p were $-0.462^{*}-$, $-0.497^{*}-$, $-0.496^{*}-$, $-0.499^{*}-$, $-0.475^{*}-$ and $-0.476^{*}-$ for ^{40}Ca, ^{48}Ca, ^{90}Zr, ^{116}Sn, ^{144}Sm and ^{208}Pb nuclei, respectively are small (weak). From Fig.6, It can be concluded that the impact of the symmetry energy density J on neutron radii (J$\rightarrow$R$_n$) is weaker than that of R_p (J$\rightarrow$R$_p$) or nonexistent. In general, from Figs.5 and 6, there is an influence of two nuclear matter properties (J and K_{NM}) on proton and neutron radii in a space of Skyrme functional, we demonstrate the existence of a relation between (K_{NM} $\rightarrow$R$_n$ and R_p) for all the investigated nuclei except for ^{40}Ca and ^{48}Ca ($K_{NM}\rightarrow$R$_n$) it is weak. This illustrates that these quantities are coupled by the skyrme force and higher than (J$\rightarrow$R$_n$, R_p), where the relation (J$\rightarrow$R$_n$) is smaller (weaker) than (J$\rightarrow$R$_p$).

4. Conclusions:

In this study, the effect of incompressibility modulus K_{NM} and symmetry energy density J on charge distribution and root-mean-square radii of neutron R_n and proton R_p has been investigated for light, medium and heavy closed-shell nuclei $^{40,48}Ca$, ^{90}Zr, ^{116}Sn, ^{144}Sm and ^{208}Pb within the framework of self-consistent Hartree-Fock (HF) with 20 types of Skyrme interaction. Good agreements were obtained between our HF results of charge density distribution for all of the used types of Skyrme interaction with the experimental data at the surface and interior regions, while our results underestimated the experimental data line inside the investigated nuclei for SVII, SIII, QMC2 and GS2 sets. Concerning, the sensitivity of proton and neutron root-mean-square radii to nuclear matter properties, we conclude there is an impact of the incompressibility K_{NM} on R_n and R_p. Also, it can be concluded that the impact of the symmetry energy density J on neutron radii (J $\rightarrow$R$_n$) is weaker than that of R_p (J $\rightarrow$R$_p$) or nonexistent.

Funding: None.

Data Availability Statement: All of the data supporting the findings of the presented study are available from corresponding author on request.

Declarations:

Conflict of interest: The authors declare that they have no conflict of interest.

Ethical approval: The manuscript has not been published or submitted to another journal, nor is it under review.

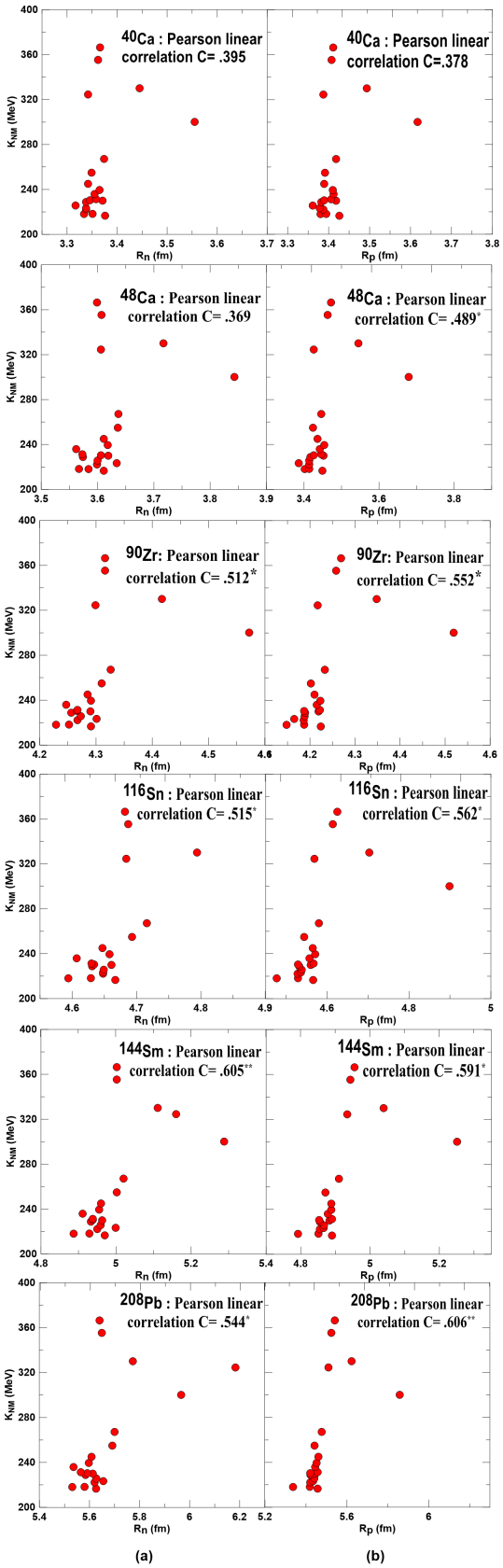

Figure 5. Incompressibility K_{NM} of ^{40}Ca, ^{48}Ca, ^{90}Zr, ^{116}Sn, ^{144}Sm and ^{208}Pb nuclei as a function of (a) R_n and (b) R_p.

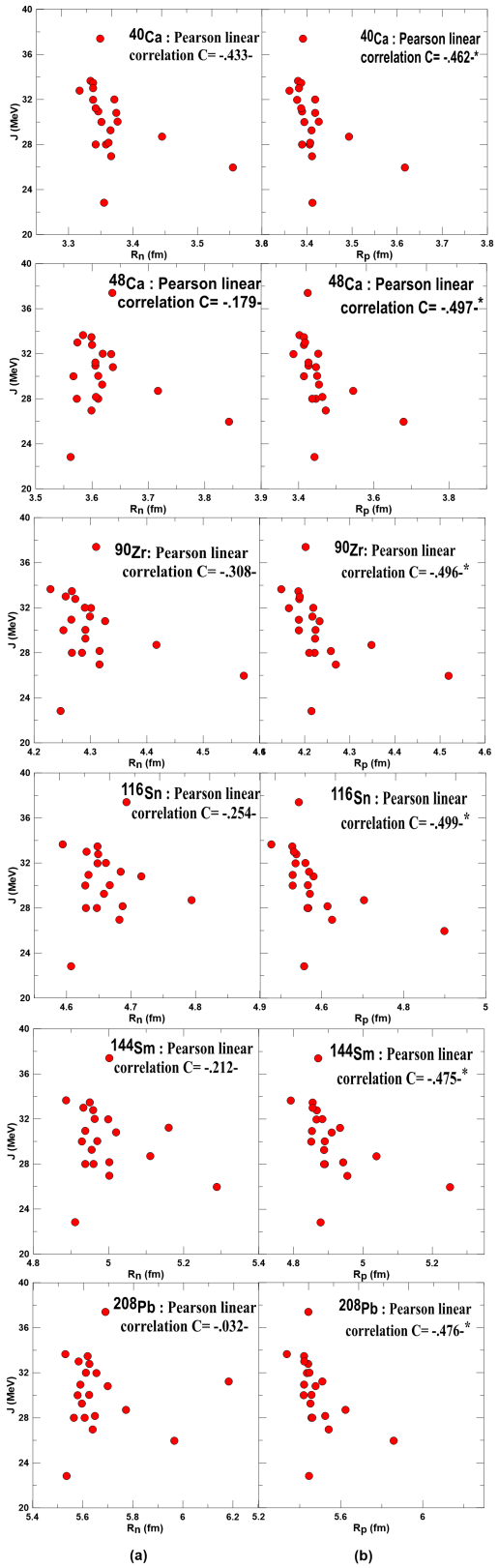

Figure 6. Symmetry energy J of ^{40}Ca, ^{48}Ca, ^{90}Zr, ^{116}Sn, ^{144}Sm and ^{208}Pb nuclei as a function of (a) R_n and (b) R_p.

References

[1] P. Ring and P. Schuck. *The Nuclear Many-Body Problem*. New York: Springer-Verlag, 1980.

[2] K. S. Krane. *Introductory Nuclear Physics*. Wiley, United State of America, 2nd edition, 1988.

[3] Ali H. Taqi and E. G. Khidher. Nuclear multipole excitations in the framework of self-consistent hartree–fock random phase approximation for skyrme forces. *Pramana-Journal Physics*, 93:60, 2019.

[4] Ali H. Taqi and G. I. Alawi. Isoscalar giant resonance in $^{100,116,132}sn$ isotopes using skyrme hf-rpa. *Journal of clinical lipidology*, A983:103, 2019.

[5] Ali H. Taqi and Malik A. Hasan. Ground-state properties of even–even nuclei from he (z = 2) to ds (z = 110) in the framework of skyrme–hartree–fock–bogoliubov theory. *Arabian Journal for Science and Engineering*, 47:761–775, 2022.

[6] Ali H. Taqi and Safa M. Qatal. Nuclear structure of samarium isotopes using skyrme and gogny hartree–fock–bogoliubov method. *Iranian Journal of Science and Technology, Transaction A: Science*, 46:967, 2020.

[7] Ali H. Taqi and Abdullah H. Ibrahim. Collective excitations of ^{14}n and ^{10}b nuclei. *Kirkuk University Journal-Scientific Studies*, 11(1):202, 2016.

[8] I. Angeli and K.P. Marinova. Table of experimental nuclear ground state charge radii: an update. *Atomic Data and Nuclear Data Tables*, 99(1):69, 2013.

[9] Junjie Yang and J. Piekarewicz. Difference in proton radii of mirror nuclei as a possible surrogate for the neutron skin. *Physical Review*, C97:014314, 2018.

[10] H. De Vries, C. W. de Jager, , and C. De Vries. Nuclear charge-density-distribution parameters from elastic electron scattering. *Atomic Data and Nuclear Data Tables*, 36:495, 1987.

[11] S. Typel and B. A. Brown. Neutron radii and the neutron equation of state in relativistic models. *Physical Review*, C64:027302, 2001.

[12] P. Danielewicz. Surface symmetry energy. *Nuclear Physics*, A727:233, 2003.

[13] M. Kortelainen, J. Erler, W. Nazarewicz, N. Birge, Y. Gao, and E. Olsen. Neutron-skin uncertainties of skyrme energy density functionals. *Physical Review*, C 88:031305(R), 2013.

[14] P.-G. Reinhard and W. Nazarewicz. Nuclear charge and neutron radii and nuclear matter: Trend analysis in skyrme density-functional-theory approach. *Physical Review*, C 93:051303(R), 2016.

[15] B. A. Brown. Neutron radii in nuclei and the neutron equation of state. *Physical Review Letters*, 85:5296, 2000.

[16] R. Furnstahl. Neutron radii in mean-field models. *Nuclear Physics*, A 706:85, 2002.

[17] P.-G. Reinhard and W. Nazarewicz. Information content of a new observable: The case of the nuclear neutron skin. *Physical Review*, C 81:051303, 2010.

[18] F. J. Fattoyev and J. Piekarewicz. Has a thick neutron skin in ^{208}pb been ruled out. *Physical Review Letters*, 111:162501, 2013.

[19] J. Piekarewicz, B. K. Agrawal, G. Colò, W. Nazarewicz, N. Paar, P.-G. Reinhard, X. Roca-Maza, , and D. Vretenar. Electric dipole polarizability and the neutron skin. *Physical Review*, C85:041302, 2012.

[20] X. Roca-Maza, M. Centelles, X. Viñas, and M. Warda. Neutron skin of ^{208}pb, nuclear symmetry energy, and the parity radius experiment. *Physical Review Letters*, 106:252501, 2011.

[21] W. Nazarewicz, P.-G. Reinhard, W. Satuła, and D. Vretenar. Symmetry energy in nuclear density functional theory. *European Physical Journal A*, 50:20, 2014.

[22] Ali H. Taqi and M. S. Ali. Self-consistent hartree-fock rpa calculations in ^{208}pb. *Indian Journal of Physics*, 92:69, 2017.

[23] T. H. R. Skyrme. The effective nuclear potential. *Nuclear Physics*, 9:615, 1959.

[24] D. Vautherin and D. M. Brink. Hartree-fock calculations with skyrme's interaction. i. spherical nuclei. *Kirkuk University Journal/Scientific Studies*, C5 (1972):626, 1959.

[25] M. Bender, P.-H. Heenen, and P.-G. Reinhard. Self-consistent mean-field models for nuclear structure. *Reviews of Modern Physics*, 75:121, 2003.

[26] J. R. Stone and P. G. Reinhard. The skyrme interaction in finite nuclei and nuclear matter. *Progress in Particle and Nuclear Physics*, 58(2):587, 2007.

[27] Ali H. Taqi and Zainab Q. Mosa. Nuclear structure of zirconium isotopes $^{90,96,106}zr$ using skyrme hf-rpa. *Egyptian Journal of Physics*, 48:1, 2020.

[28] Ali H. Taqi and Ebtihal G. Khider. Ground and transition properties of ^{40}ca and ^{48}ca nuclei. *Nuclear Physics and Atomic Energy*, 19:326, 2018.

[29] Ali H. Taqi. A visual fortran 90 program for the two-particle or two-hole excitations of nuclei: The pprpa program. *SoftwareX*, 5:51, 2016.

[30] J. Bartel, P. Quentin, M. Brack, C. Guet, and H.B. Hakansson. Toward a better parametrisation of skyrme-like effective forces: A critical study of the skm* force. *Nuclear Physics*, A386:79, 1982.

[31] S. Shlomo, V. M. Kolomietz, and G. Colo. Deducing the nuclear-matter incompressibility coefficient from data on isoscalar compression modes. *European Physical Journal*, A30:23, 2006.

[32] P. Klupfel, P.-G. Reinhard, T. J. Burvenich, and J. A. Maruhn. Variations on a theme by skyrme: A systematic study of adjustments of model parameters. *Physical Review*, C79:034310, 2009.

[33] P.-G. Reinhard, D. J. Dean, W. Nazarewicz, J. Dobaczewski, J. A. Maruhn, and M. R. Strayer. Shape coexistence and the effective nucleon-nucleon interaction. *Physical Review*, C 60:014316, 1999.

[34] A.W. Steiner, M. Prakash, J. M. Lattimer, and P. J. Ellis. Isospin asymmetry in nuclei and neutron stars. *Physics Reports*, 411:325, 2005.

[35] M. N. Harakeh and A. van der Woude. *Giant Resonances*. Oxford Science Publications, 2001.

[36] J. C. Mavropoulos, W. S. Yancy, J. Hepburn, and E. C. Westman. Tensor part of the skyrme energy density functional: Spherical nuclei. *Physical Review*, C76:014312, 2007.

[37] Zhen Zhang, Yeunhwan Lim, Jeremy W. Holt, and Che Ming Ko. Nuclear dipole polarizability from mean-field modeling constrained by chiral effective field theory. *Physics Letters*, B777:73, 2018.

[38] J. M. Pearson and S. Goriely. Isovector effective mass in the skyrme-hartree-fock method. *Physical Review*, C64:027301, 2001.

[39] M. Onsi, H. Przysiezniak, and J. M. Pearson. Dequation of state of homogeneous nuclear matter and the symmetry coefficient. *Physical Review*, C 50:460, 1994.

[40] M. Rayet, M. Amould, E Tondeur, and G. Paulus. Nuclear force and the properties of matter at high temperature and density. *Astronomy Astrophysics*, 116:183, 1982.

[41] X. Roca-Maza, G. Colo, and H. Sagawa. New skyrme interaction with improved spin-isospin properties. *Physical Review*, C 86:031306, 2012.

[42] B. K. Argawal, S. Shlomo, and V. Kim Au. Nuclear matter incompressibility coefficient in relativistic and nonrelativistic microscopic models. *Physical Review*, C68 (2003):031304, 2003.

[43] Yongli Xu, Hairui Guo, Yinlu Han, and Qingbiao Shen. New skyrme interaction parameters for a unified description of the nuclear properties. *Journal of Physics G: Nuclear and Particle Physics*, 41:015101, 2014.

[44] Q. B. Shen, Y. L. Han, and H. R. Guo. Isospin dependent nucleon-nucleus optical potential with skyrme interactions. *Physical Review*, C80:024604, 2009.

[45] B. A. Brown, G. Shen, G. C. Hillhouse, J. Meng, and A. Trzcińska. Neutron skin deduced from antiprotonic atom data. *Physical Review*, C76:034305, 2007.

[46] P. A. M. Guichon and A. W. Thomas. Quark structure and nuclear effective forces. *Physical Review Letters*, 93:13, 2004.

[47] M. J. Giannoni and P. Quentin. The mass parameter in the generator coordinate method. *Physical Review*, C21:2076, 1980.

[48] M. Dutra, O. Lourenco, J. S. Sa Martins, and A. Delfino. Skyrme interaction and nuclear matter constraints. *Physical Review*, C85:035201, 2012.

[49] J. Zenihiro, H. Sakaguchi, S. Terashima, T. Uesaka, G. Hagen, M. Itoh, T. Murakami, Y. Nakatsugawa, T. Ohnishi, H. Sagawa, H. Takeda, M. Uchida, H.P. Yoshida, S. Yoshida, and M. Yosoi. Direct determination of the neutron skin thicknesses in ^{4048}Ca from proton elastic scattering at ep=295 mev. *arXiv*, 1810:11796, 2018.

[50] H. de Vries, C.W. de Jager, and C. de Vries. Nuclear charge-density-distribution parameters from elastic electron scattering. *Atomic Data and Nuclear Data Tables*, 36:495, 1987.

تأثير عدم الانضغاطية والتناظر كثافة الطاقة على توزيع الشحنات وأنصاف أقطار نوى مغلقة الغلاف

[1*] شيماء حسين امين، [2] احمد عزيز احمد، [3] علي حسين تقي

[2,1*] قسم الفيزياء، كلية العلوم، الجامعة المستنصرية، بغداد، العراق.

[3] قسم الفيزياء، كلية العلوم، جامعة كركوك، كركوك، العراق.

[*] **الباحث المسؤول:** *shaymaahussein7988@yahoo.com*

الخلاصة

في العمل الحالي ، تم التحقق من تأثير معامل عدم الانضغاط K_{NM} وكثافة طاقة التناظر J على توزيع الشحنة ونصف قطر الجذر التربيعي للنيوترون R_n والبروتون R_p لمجموعة واسعة من انوية الذرات مغلقة الغلاف الخفيفة والمتوسطة والثقيلة $^{40}_{20}Ca_{20}$ ، $^{48}_{20}Ca_{28}$ ، $^{90}_{40}Zr_{50}$ ، $^{116}_{50}Sn_{66}$ ، $^{144}_{62}Sm_{82}$ و $^{208}_{62}Pb_{126}$ في إطار تقريب $Hartree-Fock(HF)$ المتسق ذاتيًا مع 20 نوعًا من تفاعلات *Skyrme* التي لها مجموعة واسعة من الخصائص النووية مثل معامل عدم الانضغاط K_{NM} وكثافة طاقة التناظر J . تم الحصول على كثافات الشحنة النووية ومقارنتها مع البيانات التجربة لكي تعطينا صورة عن البنية الداخلية للانوية التي تم فحصها. كما تم دراسة العلاقة بين نصف قطر الجذر التربيعي للبروتون والنيترون مع خصائص المادة النووية والتي شملت معامل عدم الانضغاط K_{NM} وكثافة طاقة التناظر J من خلال ايجاد ومناقشة معامل ارتباط بيرسون الاحصائي الخطي لغرض المساعدة في صياغة التفاعل النووي.

الكلمات الدالة:

تقريب $Hartree-Fock(HF)$ ، تفاعل *Skyrme* ، توزيع الشحنة، انصاف اقطار الجذر التربيعي.

التمويل: لايوجد.

بيان توفر البيانات: جميع البيانات الداعمة لنتائج الدراسة المقدمة يمكن طلبها من المؤلف المسؤول.

اقرارات:

تضارب المصالح: يقر المؤلفون أنه ليس لديهم تضارب في المصالح.

الموافقة الأخلاقية: لم يتم نشر المخطوطة أو تقديمها لمجلة أخرى، كما أنها ليست قيد المراجعة.